# Binding of a Myristoylated Protein to the Lipid Membrane Influenced by Interactions with the Polar Head Group Region

## ELECTRONIC SUPPORTING INFORMATION

Izabella Brand,[1]*, Dorota Matyszewska[2] and Karl-Wilhelm Koch[3]

[1] Department of Chemistry, University of Oldenburg, D-26111 Oldenburg, Germany

[2] Faculty of Chemistry, Biological and Chemical Research Centre, University of Warsaw, ul. Żwirki i Wigury 101, 02-089 Warsaw, Poland

[3] Department of Neuroscience, University of Oldenburg, D-26111 Oldenburg, Germany

Content:



[1]* To whom correspondence should be addressed, I. Brand: izabella.brand@uni-oldenburg.de (phone: 0049-441-798-3973, Fax: 0049-441-798-3979 )

## SI.1 Structure of recoverin and DMPC molecule

The neuronal calcium sensor protein recoverin has covalently attached acyl groups, mainly myristoyl (C14:0), at the N-terminus.[1] The intracellular binding of $Ca^{2+}$ occurs at EF-hand motifs.[2] A prototypical EF hand motif contains ca. 40 amino acids, which form two short α-helical fragments linked via a loop structure. Figure SI.1 shows the structure of recoverin (PDB: 1JSA) [3] in the $Ca^{2+}$ bound state. Recoverin contains 4 EF-hand motifs but only EF-hand 2 and 3 are functional $Ca^{2+}$ binding sites.[4]

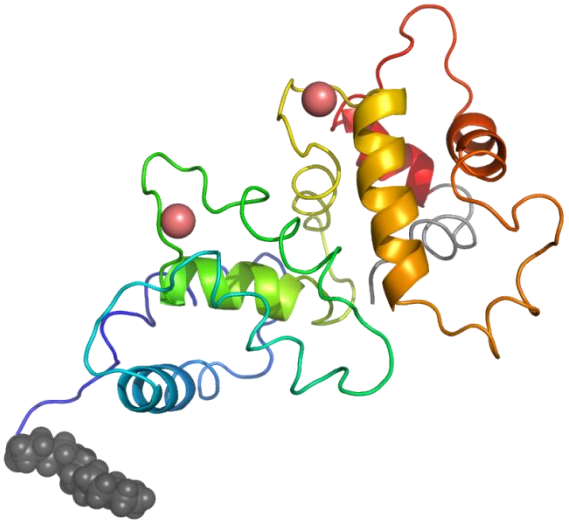

**Figure SI.1** The structure of recoverin (1JSA) with four EF hand motifs marked in blue, green, yellow and red.

1,2-dimyristoyl-*sn*-glycero-3-phosphatidylcholine (DMPC) is a zwitterionic phospholipid. The structure of DMPC molecule is shown in Figure SI.2.

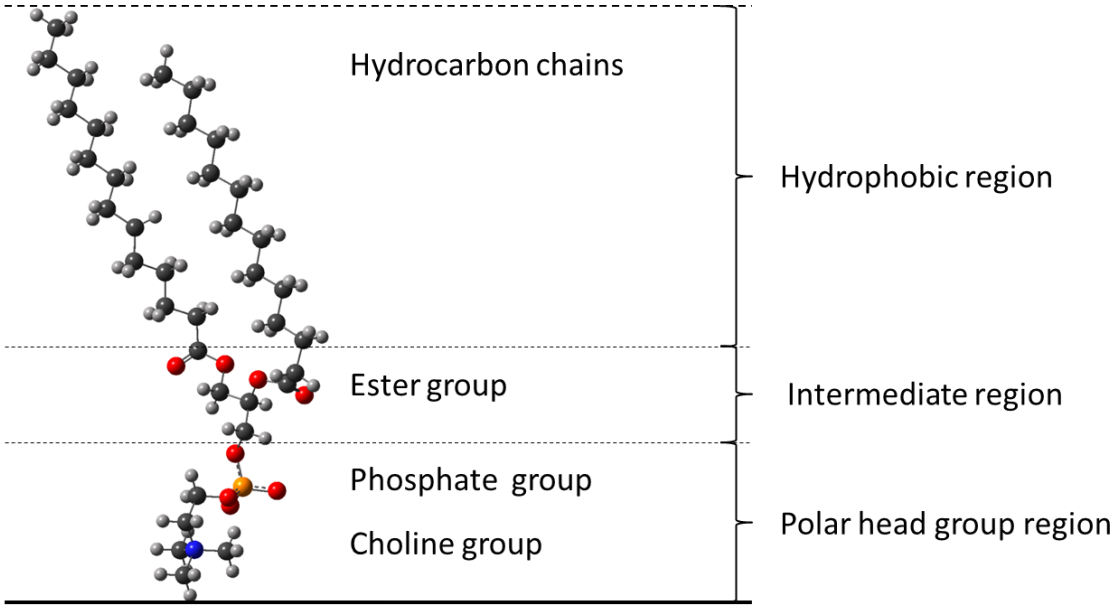


**Figure SI.2** The structure of a DMPC molecule, atom coordinates were taken from A-DMPC crystal structure [5].

The lipid molecule contains two myristoyl chains (C14) which compose the hydrophobic fragment of the amphiphilic molecule. The phosphatidylcholine moiety composes the polar head group of the lipid molecule. The ester group is present in the intermediate region and connects the hydrophobic and hydrophilic fragments. In this work we analyze the hydration and orientation of the carbonyl ester group in DMPC molecule during interaction of the lipid molecules in a model lipid bilayer with recoverin. The transition dipole vector of the ν(C=O) group lies along the C=O bond, showing the orientation of the carbonyl ester group in the lipid molecule.[6]

**SI.2 Surface pressure – time plot of lipid monolayer interacting with recoverin**

Figure SI.3 shows a surface pressure vs. time plot recorded during interaction of 2 μM recoverin in the electrolyte solution with the DMPC:cholesterol monolayer at the liquid|air interface.

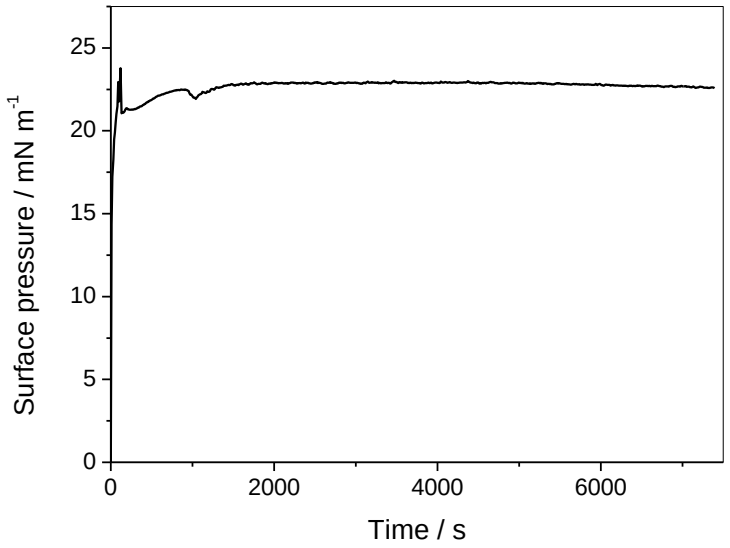


**Figure SI.3** Surface pressure vs. time plot recorded during interaction of 2µM recoverin with DMPC:cholesterol monolayer at the air| aqueous electrolyte 50 mM $NaNO_3$, 2mM $Ca(NO_3)_2$ interface.

To observe the impact of the protein interaction with the lipid monolayer, the surface pressure of the electrolyte solution containing recoverin was set to zero ($\pi_0$ = 0.05 mN $m^{-1}$). Afterwards, few drops of DMPC:cholesterol mixture were added onto the liquid|air interface. During the interaction with recoverin the surface pressure increases to equilibrium surface pressure $\pi_e$ = 22.5 mN $m^{-1}$. This value is in excellent agreement with the $\pi_e$ = 20 mN $m^{-1}$ measured by Calvez et al. [7] for DMPC and DSPC monolayers interacting with recoverin. The $\pi_e$ of recoverin is close to 15 mN $m^{-1}$.[8] The difference in the increase in the surface pressure shown in figure SI.3 is $\Delta\pi$ = 22 mN $m^{-1}$. It is higher than the $\pi_e$ of recoverin and in agreement with literature[7, 9] and indicates that the protein binding to the lipid monolayer is governed by hydrophobic as well as charge-charge and charge-dipole interactions in addition to the protein surface activity.

**SI.3 Selection of experimental conditions in *in situ* spectroelectrochemical experiments**

*In situ* analysis of the structure of biologically relevant supramolecular assemblies such as models of cell membranes (such as lipid-protein assemblies) brings new experimental requirements. The combination of experimental conditions of PM IRRAS with

electrochemical control to experimental conditions required to maintain the biological activity of biomolecules limits the application of *in situ* PM IRRAS.

A proper selection of the electrolyte solution for these experiments has a crucial role. The stability of biomolecules cannot be affected by ions present in the electrolyte solution. The use of aqueous, buffered electrolytes with physiological pH and a constant temperature (usually 37 °C) is often essential to preserve the physiological activity of biomolecules. Chloride ions are commonly present in body fluids. However, the $Cl^-$ ions adsorb strongly on gold, platinum and silver surfaces.[10-12] Since the number of materials available as electrodes and mirrors for IR radiation is limited to metals such as Au, Pt, Ag, Cu the use of electrolyte solutions containing ions which specifically adsorb on their surfaces (e.g. $Cl^-$) is not possible. Therefore, NaF is often used as electrolyte in *in situ* PM IRRAS experiments. However, $F^-$ ions are toxic for many biomolecules and may lead to a denaturation, conformation and activity change of proteins. For this reason they were not used in our experiments.

In addition, some ions present in the electrolyte solution (*e.g.* $NO_3^-$, $ClO_4^-$, $SO_4^{-2}$) absorb the IR radiation. A strong absorption of the IR light by the electrolyte may overlap with the usually weak absorption originating from a biomimetic film and the IR absorption signal from the sample cannot be distinguished from the strong absorption by the electrolyte ions. $NO_3^-$ ions adsorb weakly on the Au surface.[13] They absorb the IR light in 1420-1320 $cm^{-1}$ and 1080-1040 $cm^{-1}$ spectral regions. These spectral regions do not interfere with the absorption modes of the amide I mode in proteins and with C=O stretching, CH stretching and CH bending modes of phosphatidylcholines. In addition, $Ca(NO_3)_2$ is soluble in water. The presence of $Ca^{2+}$ ion is necessary for the interaction of recoverin with the lipid molecules in the membrane. For these reasons 50 mM $NaNO_3$, 2mM $Ca(NO_3)_2$ is used as the electrolyte solution.

## SI. 4 2-dimensional correlation spectroscopy of the amide I' mode region of recoverin bound to the membrane surface

The second derivative of the amide I' region of the PM IRRA spectra of membrane bound Rv and n-Rv give three IR absorption maxima at 1644-49 $cm^{-1}$, 1666 $cm^{-1}$ and the weak one at 1678 $cm^{-1}$. A weak shoulder around 1633-30 $cm^{-1}$ is seen in the second derivative plots. Two-dimensional correlation spectroscopy (2DCS) is a complementary to the second derivative

analytical method of the deconvolution of overlapped IR absorption modes.[14] PM IRRA spectra in the negative-going potential scan are used to perform the correlation and analyze potential dependent changes in the secondary structure elements of recoverin as a function of the applied potential.

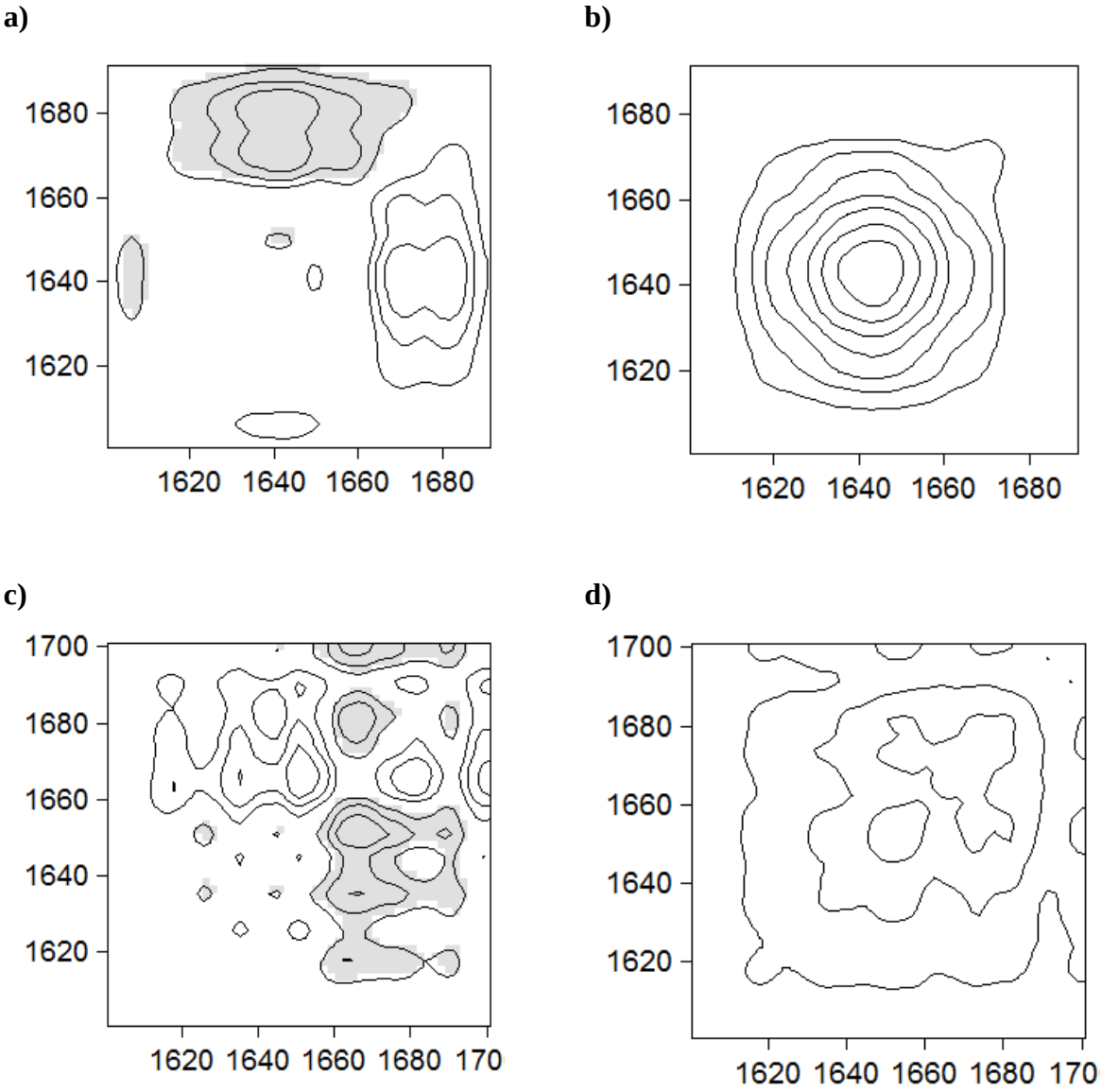


**Figure SI.4** a,c) Asynchronous and b,d) synchronous 2-DCS spectra of the amide I' mode of a,b) n-recoverin and c,d) recoverin bound to the DMPC:cholesterol bilayer on the Au electrode surface.

Asynchronous spectra are characterized by the presence of cross peaks (symmetric with respect to the diagonal). They facilitate the deconvolution of overlapped IR absorption modes. The asynchronous 2DC spectrum of n-Rv shows cross peaks at 1648, 1665 and 1679 $cm^{-1}$

(Figure SI.4 a). The asynchronous 2DC spectrum of Rv is more complex than that of n-Rv. It shows cross peaks at 1640, 1650, 1666 and 1682 $cm^{-1}$. The deconvolution of the amide I' mode region indicates that α-helices (1640-50 $cm^{-1}$), β-turns (1679 $cm^{-1}$) and disordered (1665 $cm^{-1}$) structural elements belong to the recoverin structure. In membrane bound Rv the α-helices give two contributions to the asynchronous 2DC spectrum (1640 and 1650 $cm^{-1}$). It indicates that the strength of hydrogen bonds formed to α-helices change as a function of potential applied to the gold electrode. It may also indicate some changes in the conformation and mobility of the α helical fragments in Rv.

In synchronous spectra peaks appear in the diagonal and indicate structural, conformational changes occurring during the applied perturbation. In our case the perturbation is the potential applied to the Au electrode. The synchronous spectrum of n-Rv shows an autocorrelation peak at 1647 $cm^{-1}$ (Figure SI.4b), indicating that α-helical structural elements are affected in the potential scan. The synchronous spectrum of Rv bound to the lipid membrane shows autocorrelation peaks at 1650 $cm^{-1}$ and ca. 1660 – 1678 $cm^{-1}$ (Figure SI.4d). These peaks lie on the diagonal and indicate that IR absorption modes of the entire protein change during the potential scan.

## SI.5 Correlation between the intensity of an IR absorption band in IRRAS and orientation of a molecule in an anisotropic film

According to the surface selection rule of infrared reflection absorption spectroscopy (IRRAS)[15], in an isotropic film, the intensity of an IR absorption mode depends on the surface concentration of molecules in this film ($\Gamma$) and on the orientation of the transition dipole vector of a given absorption mode ($\vec{\mu}$) vs. electric field vector ($\vec{E}$) (always perpendicular to the surface, see Figure SI 5)[16]:

$$\int Ad\nu \propto \Gamma\left|\vec{\mu}\bullet\vec{E}\right|^2 = \Gamma\left|\vec{\mu}\right|^2\left|\vec{E}\right|^2\cos^2\theta \qquad \text{(SI.1)},$$

where $\theta$ is the angle between $\vec{\mu}$ and $\vec{E}$ vectors.

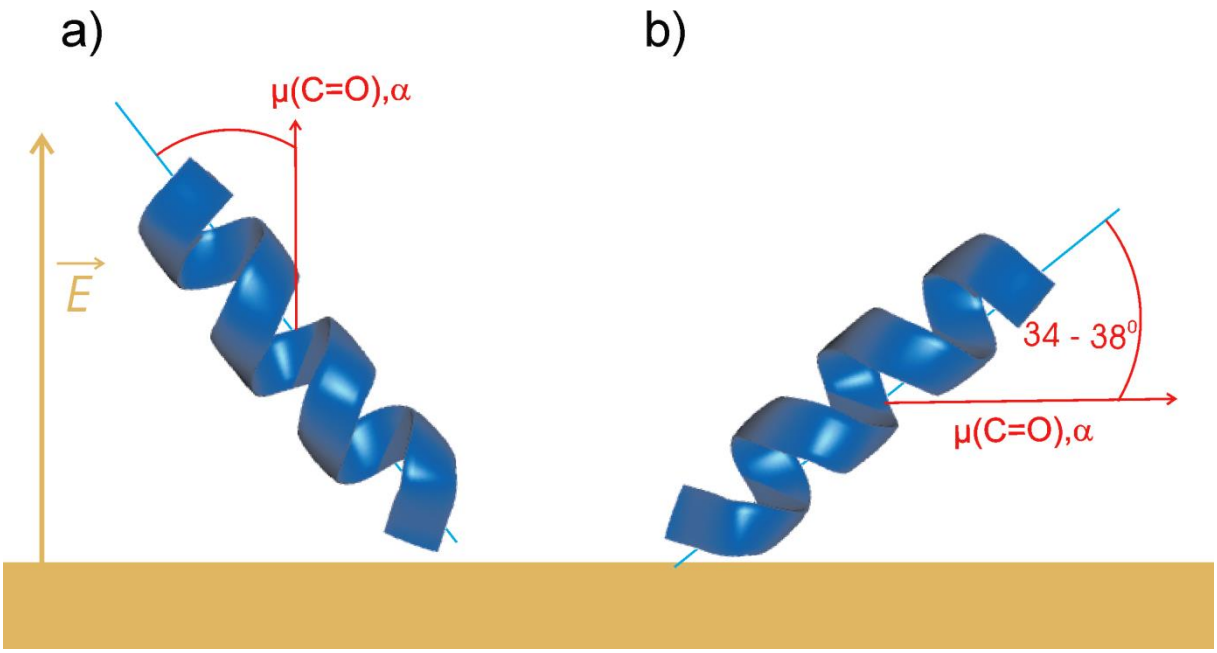


**Figure SI.5** Limiting cases for the orientation of the α-helical fragment in a protein adsorbed on a solid surface. A blue line shows the direction of the long axis of the α-helix. The direction of the transition dipole vector of the amide I mode (red arrow) and the direction of the electric field vector of the *p*-polarized light at the phase boundary (gold arrow) are shown in the figure.

Depending on the value of $\theta$, and thus on the orientation of a molecule in the studied film, some IR absorption bands may be enhanced while others may disappear from the IRRA spectrum. Figure SI.5 shows two limiting cases for the orientation of a α-helical fragment in a protein adsorbed on a solid surface leading to the enhancement and cancellation of the amide I mode in the IRRA spectrum. A parallel orientation of $\vec{\mu}$ and $\vec{E}$ vectors causes their strong coupling and thus the intensity of the IR absorption band of the amide I mode is enhanced (Figure SI.5a). When the angle between $\vec{\mu}$ and $\vec{E}$ vectors is equal to 90º (Figure SI.5b), according to eq. SI.1, the integral intensity of the amide I mode is equal to zero. In this case there is no coupling of the transition dipole and the electric field vectors.

**SI.6 IRS transmission spectrum of recoverin in solution phase**

The amide I' mode region of the transmission IR spectrum is used to determine the secondary structure elements of Rv dissolved in 0.05 M $NaNO_3$ with 2 mM $Ca(NO_3)_2$ electrolyte solution (Figure SI.6).

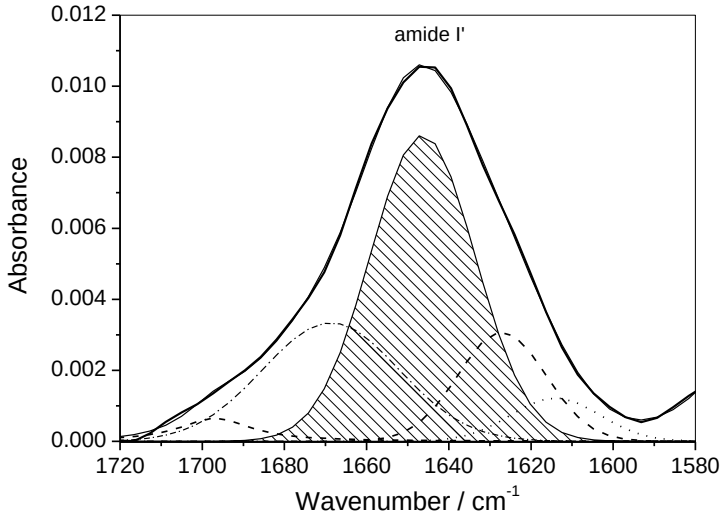


**Figure SI.6** Deconvoluted FT IR spectrum (thick line) of myr-recoverin in the amide I' mode spectral region ($1 \times 10^{-4}$ M) in 50 mM $NaNO_3$, 2 mM $Ca(NO_3)_2$ in $D_2O$.

The amide I' mode of recoverin is deconvoluted into five modes centered at: 1682, 1667, 1648, 1628 and 1615 $cm^{-1}$. This result is in a very good agreement with study by Potvin-Fournier *et al.*[17]. The strongest mode is centered at 1648 $cm^{-1}$. It is ascribed to the α-helical structural elements. It consists 52 % of the total amide I' mode intensity, corresponding well to α-helix content in myristoylated recoverin in $Ca^{2+}$ bound state.[3] The amide I' mode at 1666 $cm^{-1}$ is ascribed to disordered, flexible structural elements in the protein.[17] The high frequency contribution to the amide I' mode at 1682 $cm^{-1}$ arises from β-turns. Moreover, recoverin contains four short antiparallel β-sheet strands.[18] A weak mode at 1628 $cm^{-1}$ is assigned to the β-sheet structure of the protein. The IR spectra of Rv indicate that the content of β-sheet structures is on the level of 15-20 %. This was significantly more than 2 – 4 % β-sheet

structures determined in NMR studies.[3] In the presence of $Ca^{2+}$ ions recoverin tends to aggregate, due to hydrophobic-hydrophobic interactions,[19-21] which lead to an increase in the content of the β-sheet structural elements.[17] Reason for this conformational transition was probably the high $Ca^{2+}$ ions and protein concentration in our electrolyte solution. The low frequency mode at 1615 $cm^{-1}$ arises from the contribution to the amide I' mode of aromatic and carboxylic groups present in the corresponding side chains.[17, 22] Concluding, the secondary structure elements determined from the IR transmission spectrum shown in Figure SI.6 are in agreement with myrisotylated and non-myristoylated recoverin in $Ca^{2+}$ bound state determined in IR, NMR and XRD experiments.[3, 4, 17, 23]

**References:**


1. Dizhoor, A. M.; Ericsson, L. H.; Johnson, R. S.; Kumar, S.; Olshevskaya, E.; Zozulya, S.; Neubert, T. A.; Stryer, L.; Hurley, J. B.; Walsh, K. A., The $NH_2$ terminus of retinal recoverin is acylated by a small family of fatty acid. *J. Biol. Chem.* **1992,** 267, (23), 16033-16036.
2. Kretsinger, R. H., Calcium coordination and the calmodulin fold: divergent versus convergent evolution. *Cold Spring Harbor Symp. Quant. Biol.* **1987,** 52, 499-510.
3. Ames, J. B.; Ishima, R.; Tanaka, T.; Gordon, J. I.; Stryer, L.; Ikura, M., Molecular mechanics of calcium-myristoyl switches. *Nature (London, U. K.)* **1997,** 389, 198-202.
4. Ames, J. B.; Porumb, T.; Tanaka, T.; Ikura, M.; Stryer, L., Amino-terminal myristoylation includes cooperative calcium binding to recoverin. *J. Biol. Chem.* **1995,** 270, 4526-4533.
5. Marsh, D., *Handbook of Lipid Bilayers*. CRC Press: New York, 2013.
6. Fringeli, U. P., The structure of lipids and proteins studied by attenuated total reflection (ATR) infrared spectroscopy. II. Oriented layers of a homologous series: Phosphatidylethanolamine to phosphatidylcholine. *Z. Naturforsch.* **1977,** 32c, 20-45.
7. Calvez, P.; Demers, E.; Boisselier, E.; Salesse, C., Analysis of the contribution of saturated and polyunsaturated phospholipid monolayers to the binding of proteins. *Langmuir* **2011,** 27, 1373-1379.
8. Desmeules, P.; Penney, S. E.; Desbat, B.; Salesse, C., Determination of the contribution of the myristoyl group and hydrophobic amino acids of recoverin on its dynamics of binding of lipid monolayers. *Biophys. J.* **2007,** 93, 2069-2082.
9. Calvez, P.; Schmidt, T. F.; Cantin, L.; Klinker, K.; Salesse, C., Phosphatidylserine allows observation of the calcium−myristoyl switch of recoverin and its preferential binding. *J. Am. Chem. Soc.* **2016,** 138, 13533-13540.
10. Clavilier, J.; Van Houng, N., Etude de la structure de la couche double sur les electrodes d'or. *J. Electroanal. Chem.* **1973,** 41, 193-199.
11. Salaita, G. N.; Lu, F.; Laguren-Davidson, L.; Hubbard, A. T., Structure and composition of the Ag(111) surface as a function of electrode potential in aqueous halide solutions. *J. Electroanal. Chem.* **1987,** 229, (1), 1-17.

12. Schwabe, K.; Schwenke, W., Untersuchungen über Anionenadsorption an Metalloberflächen in abhängigkeit vom Potential. *Electrochim. Acta* **1964,** 9, (7), 1003-1013.
13. Marinkovic, N. S.; Calvente, J. J.; Kloss, A.; Kovacova, Z.; Fawcett, W. R., SNIFTIRS studies of the electrochemical double layer Part II: Au(111) electrode in solutions with specifically adsorbed nitrate ions. *J. Electroanal. Chem.* **1999,** 467, 325-334.
14. Noda, I., Two-dimensional infrared (2DIR) spectroscopy: theory and applications. *Appl. Spectrosc.* **1990,** 44, 550-561.
15. Moskovits, M., Surface selection rules. *J. Chem. Phys.* **1982,** 77, 4408-4416.
16. Allara, D. L.; Swalen, J. D., An infrared reflection spectroscopy study of oriented cadmium arachidate monolayer films on evaporated silver. *J. Phys. Chem.* **1982,** 86, 2700-2704.
17. Potvin-Fournier, K.; Lefevre, T.; Picard-Lafond, A.; Valois-Pillard, G.; Cantin, L.; Salesse, C.; Auger, M., The thermal stability of recoverin depends on calcium binding and its myristoyl moiety as revealed by infrared spectroscopy. *Biochemistry* **2014,** 53, (1), 48-56.
18. Tanaka, T.; Ames, J. B.; Harvey, T. S.; Stryer, L.; Ikura, M., Sequestration of the membrane-targeting myristoyl group of recoverin in the calcium-free state. *Nature (London, U. K.)* **1995,** 376, 444-447.
19. Kataoka, M.; Mihara, K.; Tokunaga, F., Recoverin alters its surface properties depending on both calcium-binding and N-terminal myristoylation. *J. Biochem.* **1993,** 114, (4), 535-540.
20. Johnson Jr., W. C.; Palczewski, K.; Gorczyca, W. A.; Riazance-Lawrence, J. H.; Witkowska, D.; Polans, A. S., Calcium binding to recoverin: implications for secondary structure and membrane association. *Biochim. Biophys. Acta* **1997,** 1342, 164-174.
21. Potvin-Fournier, K.; Valois-Paillard, G.; Gagnon, M. C.; Lefevre, T.; Audet, P.; Cantin, L.; Paquin, J. F.; Salesse, C.; Auger, M., Novel approaches to probe the binding of recoverin to membranes. *Eur. Biophys. J.* **2018**.
22. Barth, A., Infrared spectroscopy of proteins. *Biochim. Biophys. Acta* **2007,** 1767, (9), 1073-1101.
23. Ozawa, T.; Fukuda, M.; Nara, M.; Nakamura, A.; Komine, Y.; Kohama, K.; Umezawa, Y., How can $Ca^{2+}$ selectively activate recoverin in the presence of $Mg^{2+}$? Surface plasmon resonance and FT-IR spectroscopic studies. *Biochemistry* **2000,** 39, 14495-14503.